Available at
www.ElsevierMathematics.com
POWERED BY SCIENCE DIRECT®
ELSEVIER Computers and Mathematics with Applications 46 (2003) 1211–1228
An International Journal
computers & mathematics with applications
www.elsevier.com/locate/camwa

Approximation and Comparison for Motion by Mean Curvature with Intersection Points

WEIZHU BAO
Department of Computational Science
National University of Singapore, Singapore, 117543
bao@cz3.nus.edu.sg

(Received March 2001; revised and accepted December 2002)

Abstract—Consider the motion of a curve in the plane under its mean curvature. It is a very interesting problem to investigate what happens when there are intersection points on the curve at which the mean curvature is singular. In this paper, we study this issue numerically by solving the Allen-Cahn equation and the nonlocal evolution equation with Kac potential. The Allen-Cahn equation is discretized by a monotone scheme, and the nonlocal evolution equation with Kac potential is discretized by the spectral method. Several curves with intersection points under motion by mean curvature are studied. From a simple analysis and our numerical results, we find that which direction to split of the curve at the intersection point depends on the angle of the curve at the point, i.e., it splits in horizontal direction when the angle $\alpha > \pi/2$, in vertical direction when $\alpha < \pi/2$, and in either direction when $\alpha = \pi/2$. © 2003 Elsevier Ltd. All rights reserved.

Keywords—Motion by mean curvature, Allen-Cahn equation, Kac potential, Nonlocal evolution equation, Intersection point.

1. INTRODUCTION

There are many natural and industrial problems in which sharp interfaces form and propagate, especially singularities and topological changes which appeared during the motion of the interfaces. Notable examples include the growth of crystalline materials, the interaction between fluid and solid, the processing and enhancement of images, the evolution of ecological systems, and the waves of excitation that occur in heart and neural tissue.

To model these and other complex phenomena, a wide variety of mathematical models have been proposed. For instance, the level set method is a successful phenomelogical model in numerically computing front propagation problems that can handle naturally singularities and topological changes such as breaking and merging [1,2]. The Allen-Cahn equation is introduced for antiphase boundary motion and motion of curve under its mean curvature [3–5]. The nonlocal evolution equation with Kac potential is proposed in studying the macroscopic behavior of the spin system with Kac potential and Glauber dynamics [6–10]. Cellular automata were used to model the formation and dynamics of patterns in a variety of chemical, biological, and ecological systems [11–14]. A diffusion-generated algorithm is proposed for motion by mean curvature [15–19].

Research supported by the National University of Singapore Grant No. R-151-000-016-112.

doi: 10.1016/S0898-1221(03)00354-7

Mathematically, we do not know rigorously what happens for the models when they are used to describe motion of a curve with intersection points under its mean curvature. On the contrary, here we study this issue numerically. The aim of this paper is to study numerically what happens to motion of a curve with intersection points under its mean curvature when using the Allen-Cahn equation and nonlocal evolution equation with Kac potential. From the numerical results, we can get hints to study the issue in a rigorous way, i.e., mathematically.

The paper is organized as follows. In Section 2, we study the issue by using the Allen-Cahn equation, including discretization and numerical results. In Section 3, we study the issue by using the nonlocal evolution equation with Kac potential. In Section 4, some conclusions are drawn.

2. THE ALLEN-CAHN EQUATION

In this section, we study numerically what happens for the Allen-Cahn equation when it is used to describe the motion of a curve with intersection points under its mean curvature.

2.1. The Equation

Let Γ_0 be a curve in $\mathbb{R}^2$. The motion of Γ_0 under its mean curvature can be described by the Allen-Cahn equation [3]

$$u_t = \triangle u + \frac{1}{\varepsilon^2} u\left(1-u^2\right), \qquad u(x,y,0) = u_0(x,y), \tag{2.1}$$

where the initial data $-1 \le u_0(x,y) \le 1$ is a monotone function near Γ_0, Γ_0 is the zero contour of $u_0(x,y)$, and ε is a small parameter. In fact, $u = \pm 1$ and $u = 0$ are stationary solutions of (2.1), and $u = \pm 1$ are stable equilibrium states, $u = 0$ is an unstable equilibrium state. The curve Γ_t, moved from Γ_0 under its mean curvature at time t, is the zero contour of the solution $u(x,y,t)$ of (2.1). The advantage of this model is that it deals with curvature implicitly. One need not compute the curvature explicitly during the motion. So it is very useful when one wants to study motion with singularities, topology changes, even with intersection points on the curve.

2.2. Discretization

To discretize equation (2.1), one needs to use a numerical method not only stable but also monotone in order to avoid incorrect solution. Here we choose the simplest method: second-order central scheme in space and forward-Euler scheme in time. Let h be the mesh size and k be the time step. The detail scheme is

$$\begin{aligned} u_{ij}^{n+1} &= u_{ij}^n + \frac{k}{h^2}\left(u_{i+1j}^n + u_{i-1j}^n + u_{ij+1}^n + u_{ij-1}^n - 4u_{ij}^n\right) + \frac{k}{\varepsilon^2} u_{ij}^n \left(1 - {u_{ij}^n}^2\right) \\ &= \left(1 - \frac{4k}{h^2} + \frac{k}{\varepsilon^2}\left(1 - {u_{ij}^n}^2\right)\right) u_{ij}^n + \frac{k}{h^2} u_{i+1j}^n + \frac{k}{h^2} u_{i-1j}^n + \frac{k}{h^2} u_{ij+1}^n + \frac{k}{h^2} u_{ij-1}^n. \end{aligned} \tag{2.2}$$

To resolve the problem spatially, the mesh size h should be less than ε, i.e., $h < \varepsilon$. It is easy to see from (2.2) that the stable and monotone condition is $k \le h^2/4$. In fact, under this CFL condition, scheme (2.2) is a positive scheme due to $-1 \le u_{ij}^n \le 1$.

The initial data is chosen as

$$u_0(x,y) = f\left(\pm \frac{d(x,y;\Gamma_0)}{\varepsilon}\right), \tag{2.3}$$

where $d(x,y;\Gamma_0)$ is the signed distance from the point (x,y) to the curve Γ_0 and $f(\cdot)$ is an odd monotone function. The plus (or minus) sign is chosen if the point (x,y) is outside (or inside) the curve Γ_0.

2.3. Direction to be Split at the Intersection Point

As shown in Figure 1, P is the intersection point, part of the initial curve Γ_0 (solid line) and grid points ('.' points) around P are depicted. Suppose that α is the angle at the intersection point P and the grid points C, Q and D, R are inside and outside Γ_0, respectively.

From the initial condition (2.3), we have

$$u_{ij}^0 = f\left(\pm\frac{d(x_i, y_j; \Gamma_0)}{\varepsilon}\right), \qquad i = 0, \pm 1, \ldots, \quad j = 0, \pm 1, \ldots. \tag{2.4}$$

From Figure 1, we have

$$|PQ| = |PR| = h, \qquad |QS| = h\sin\frac{\alpha}{2}, \qquad |RT| = h\cos\frac{\alpha}{2}, \tag{2.5}$$

where $|\cdot|$ denotes the length of the segment. This implies

$$u_{0\,0}^0 = 0, \qquad u_{-1\,0}^0 = u_{1\,0}^0 = f\left(-\frac{h\sin\alpha/2}{\varepsilon}\right), \qquad u_{0\,1}^0 = u_{0\,-1}^0 = f\left(\frac{h\cos\alpha/2}{\varepsilon}\right). \tag{2.6}$$

Substituting (2.6) into (2.2) with $n = i = j = 0$, notice that f is odd, and one obtains

$$\begin{aligned} u_{0\,0}^1 &= 0 + \frac{k}{h^2}\left[2f\left(-\frac{h\sin\alpha/2}{\varepsilon}\right) + 2f\left(\frac{h\cos\alpha/2}{\varepsilon}\right) - 0\right] + \frac{k}{h^2}0\left(1 - 0^2\right) \\ &= \frac{2k}{h^2}\left[f\left(-\frac{h\sin\alpha/2}{\varepsilon}\right) + f\left(\frac{h\cos\alpha/2}{\varepsilon}\right)\right] \\ &= \frac{2k}{h^2}\left[f\left(\frac{h\cos\alpha/2}{\varepsilon}\right) - f\left(\frac{h\sin\alpha/2}{\varepsilon}\right)\right] \\ &= \begin{cases} > 0, & 0 < \alpha < \dfrac{\pi}{2}, \\ < 0, & \dfrac{\pi}{2} < \alpha < \pi, \\ = 0, & \alpha = \dfrac{\pi}{2}. \end{cases} \end{aligned} \tag{2.7}$$

Thus, at time $t = t_1 = k$, the intersection point P is inside Γ_{t_1}, i.e., split in the horizontal direction, when $\pi/2 < \alpha < \pi$; outside Γ_{t_1}, i.e., split in vertical direction, when $0 < \alpha < \pi/2$; on Γ_{t_1} when $\alpha = \pi/2$. For the case of $\alpha = \pi/2$, the angle α at the intersection point P will be greater than $\pi/2$ to less than $\pi/2$ at some time $t > 0$ due to the motion of Γ_0 or round-off error in computer. In this case, the curve splits in either direction.

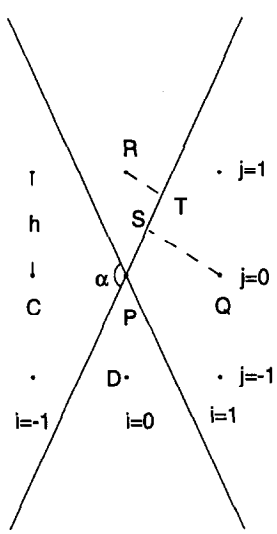

Figure 1. Part of the curve Γ_0 and grid points near the intersection point P.

2.4. Numerical Results

Using the above numerical method, we study motions of different curves Γ_0, with intersection points which are at the origin, under their mean curvatures. The problem is solved on $[-0.5, 0.5]^2$. Periodic boundary conditions are used in the computation. We choose $\varepsilon = 0.01$, the mesh size $h = 1/256$, and time step $k = 0.0000025$. In our computation, the initial data is chosen as

$$u_0(x, y) = \tanh\left(\pm\frac{d(x, y; \Gamma_0)}{\varepsilon}\right).$$

EXAMPLE 1. Motion of a circle under its mean curvature. We choose $\Gamma_0 = \{(x, y) : x^2 + y^2 = 0.4^2\}$, i.e., it is a circle centered at the origin with radius $r_0 = 0.4$. In this example, the circle will shrink to the origin and finally disappear. At time $0 \le t \le 0.08$, Γ_t is also a circle centered at the origin with radius $r = \sqrt{r_0^2 - 2t}$. Figure 2 shows the motion of Γ_0 under its mean curvature at $t_0 = 0$, $t_1 = 0.035$, $t_2 = 0.06$, $t_3 = 0.075$, $t_4 = 0.078$, and $t_5 = 0.08$. The corresponding radius of the circles are $r_0 = 0.4$, $r_1 = 0.3$, $r_2 = 0.2$, $r_3 = 0.1$, $r_4 = 0.0632$, $r_5 = 0$, respectively. From this figure, we can see Γ_0 shrinks under its mean curvature and eventually disappears.

EXAMPLE 2. Motion of a curve with an intersection point at which the angle $\alpha = \pi/2$. Figure 2 shows the motion of Γ_0 under its mean curvature at $t_0 = 0$, $t_1 = 0.001$, $t_2 = 0.004$, $t_3 = 0.008$, $t_4 = 0.012$, and $t_5 = 0.016$. From this figure, we can see Γ_0 splits at its intersection point in the vertical direction. Our numerical experiments, as well as the results in Example 5, show that the vertical break-up is unstable under discretizations. In Figure 3, as well as Figures 4–10, Γ_0 is shown in the corresponding figure with $t_0 = 0$ and the intersection point is at the origin.

EXAMPLE 3. Motion of a curve with an intersection point at which the angle $\alpha = 2\tan^{-1} 2 > \pi/2$. Figure 4 shows the motion of Γ_0 under its mean curvature at $t_0 = 0$, $t_1 = 0.001$, $t_2 = 0.004$, $t_3 = 0.008$, $t_4 = 0.012$, and $t_5 = 0.016$. From this figure, we can see Γ_0 splits at its intersection point in the horizontal direction. In fact, from our numerical experiments, we find Γ_0 always splits at its intersection point in the horizontal direction when the angle $\alpha > \pi/2$.

EXAMPLE 4. Motion of a curve with an intersection point at which the angle $\alpha = 2\tan^{-1} 1/2 < \pi/2$. Figure 5 shows the motion of Γ_0 under its mean curvature at $t_0 = 0$, $t_1 = 0.001$, $t_2 = 0.002$, $t_3 = 0.004$, $t_4 = 0.008$, and $t_5 = 0.01$. From this figure, we can see Γ_0 splits at its intersection point in the vertical direction. In fact, from our numerical experiments, we find Γ_0 always splits at its intersection point in the vertical direction when the angle $\alpha < \pi/2$.

EXAMPLE 5. Motion of a curve with an intersection point at which the angle $\alpha = \pi/2$ and a small circle, which is centered at $(0, 0.3)$ with radius r_0, near the intersection point. Figure 6 shows the motion of Γ_0 under its mean curvature at $t_0 = 0$, $t_1 = 0.001$, $t_2 = 0.004$, $t_3 = 0.008$, $t_4 = 0.012$, and $t_5 = 0.016$ with $r_0 = 0.05$ and $r_0 = 0.1$. From this figure, we can see Γ_0 splits at its intersection point in the vertical direction when $r_0 = 0.05$, i.e., in the same way as without the small circle (cf. Figure 2); and in the horizontal direction when $r_0 = 0.1$, i.e., in an opposite direction as without the small circle (cf. Figure 2). In fact, from our numerical experiments, we find Γ_0 always splits at the origin in horizontal direction when $r_0 \ge 0.095$, and in the vertical direction when the angle $r_0 \le 0.0925$.

EXAMPLE 6. Motion of a curve with an intersection point at which the angle $\alpha = 2\tan^{-1} 1/2 < \pi/2$ and a small circle, which is centered at $(0, 0.3)$ with radius r_0, near the intersection point. Figure 7 shows the motion of Γ_0 under its mean curvature at $t_0 = 0$, $t_1 = 0.001$, $t_2 = 0.002$, $t_3 = 0.004$, $t_4 = 0.008$, and $t_5 = 0.01$ with $r_0 = 0.1$. From this figure, we can see Γ_0 splits at its intersection point in the vertical direction, i.e., in the same way as without the small circle (cf. Figure 3). In fact, from our numerical experiments, we find Γ_0 always splits at the origin in the vertical direction when $\alpha < \pi/2$ even with a small circle near the intersection point.

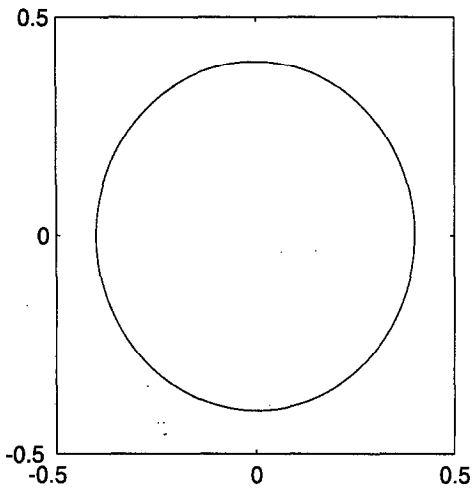

(a) $t_0 = 0$.

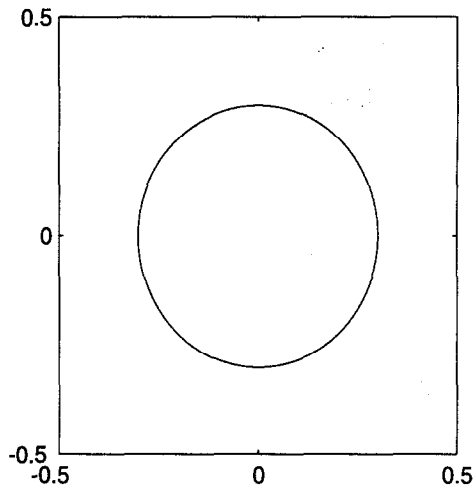

(b) $t_1 = 0.035$.

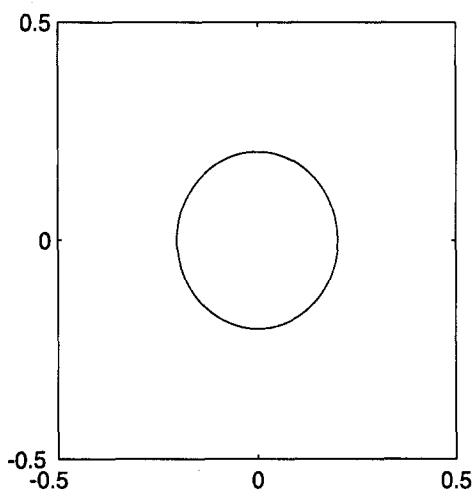

(c) $t_2 = 0.6$.

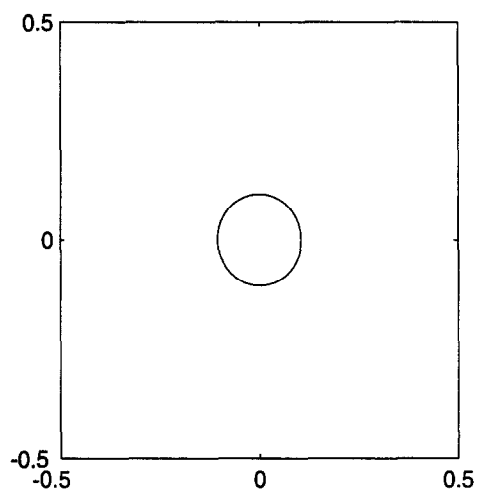

(d) $t_3 = 0.075$.

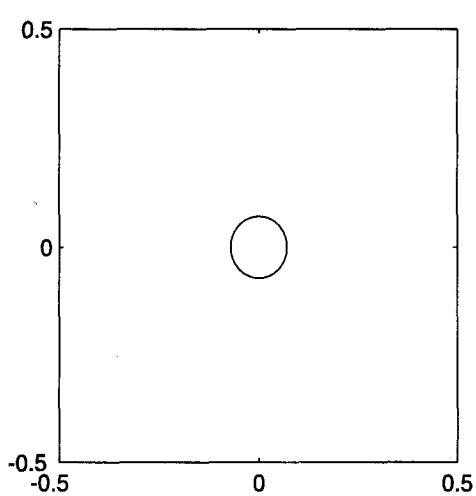

(e) $t_4 = 0.078$.

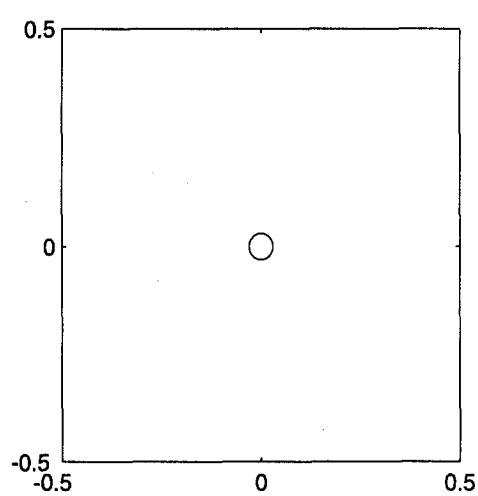

(f) $t_5 = 0.08$.

Figure 2. Numerical results for Example 1. $\varepsilon = 0.01$, $h = 1/256$, $k = 0.0000025$.

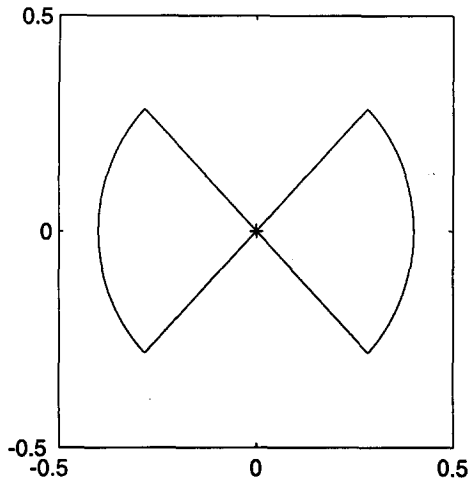

(a) $t_0 = 0$.

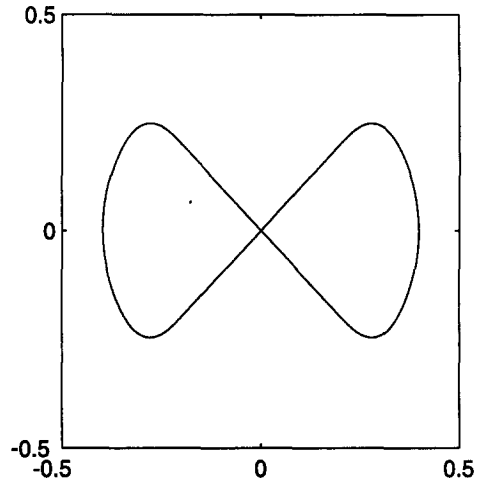

(b) $t_1 = 0.001$.

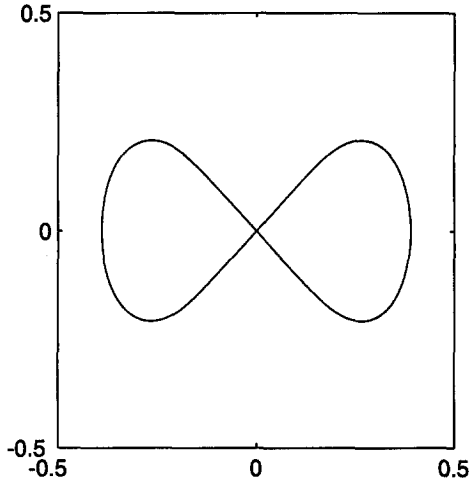

(c) $t_2 = 0.4$.

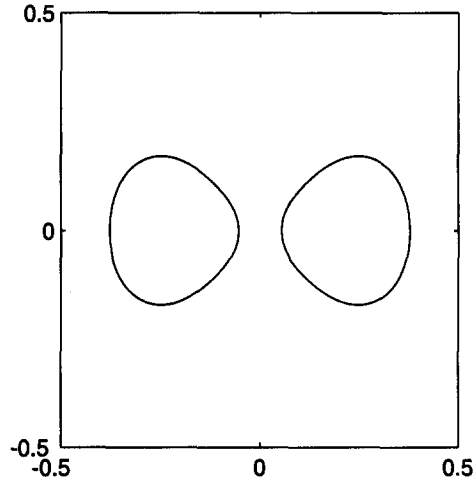

(d) $t_3 = 0.008$.

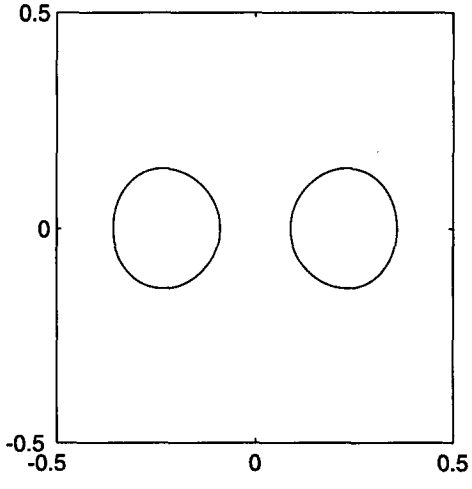

(e) $t_4 = 0.012$.

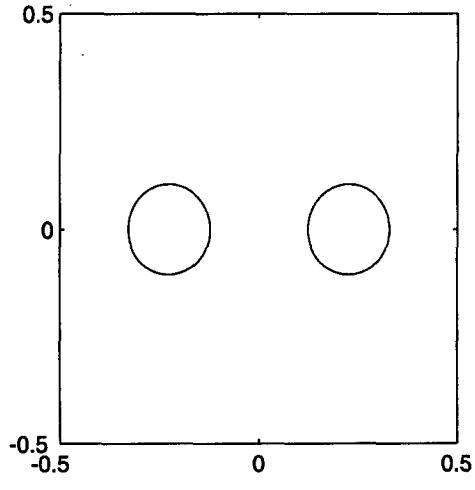

(f) $t_5 = 0.016$.

Figure 3. Numerical results for Example 2. '+' is the intersection point. $\alpha = \pi/2$, $\varepsilon = 0.01$, $h = 1/256$, $k = 0.0000025$.

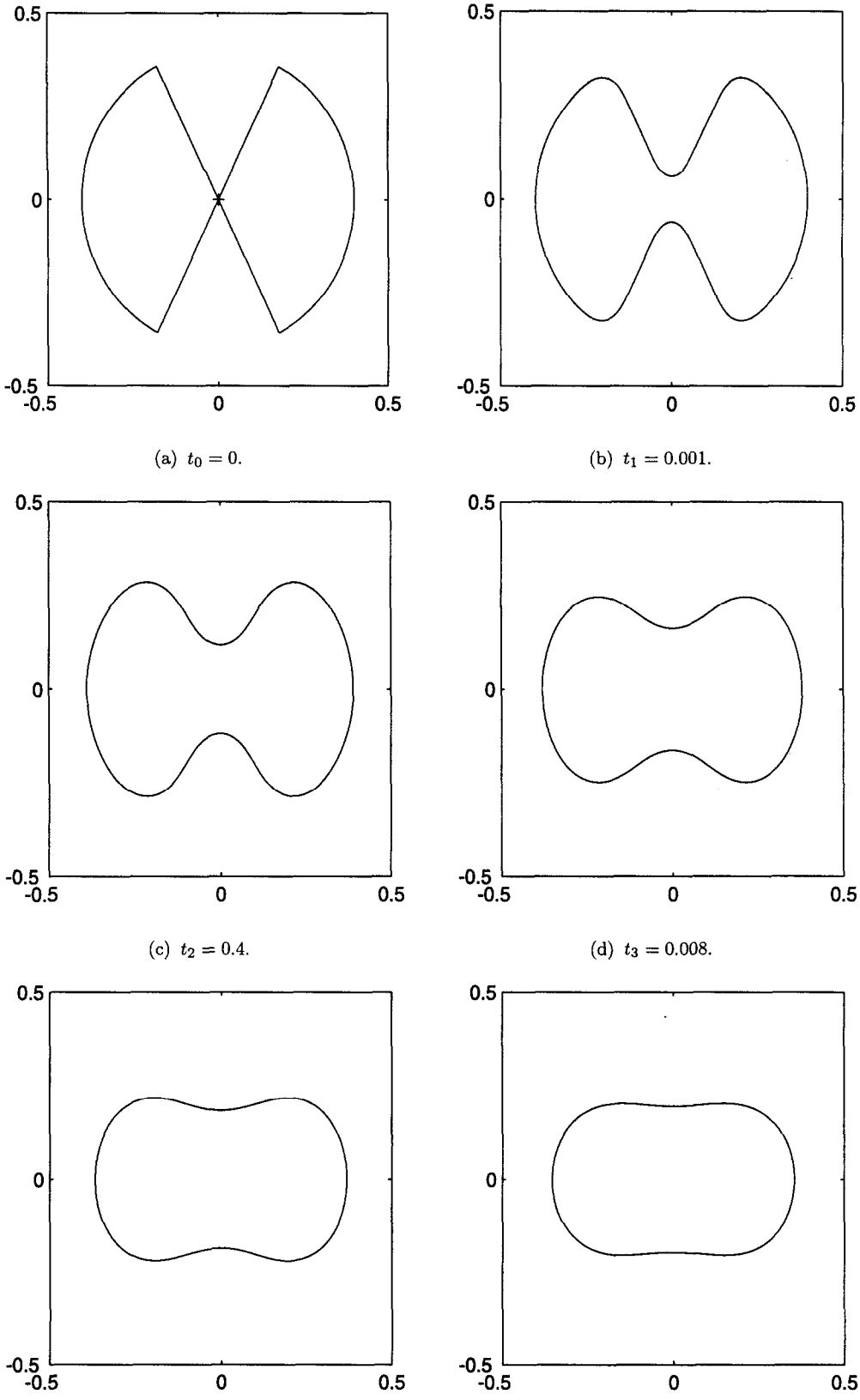

(a) $t_0 = 0$.

(b) $t_1 = 0.001$.

(c) $t_2 = 0.4$.

(d) $t_3 = 0.008$.

(e) $t_4 = 0.012$.

(f) $t_5 = 0.016$.

Figure 4. Numerical results for Example 3. '+' is the intersection point. $\alpha = 2\tan^{-1} 2 > \pi/2$. $\varepsilon = 0.01$, $h = 1/256$, $k = 0.0000025$.

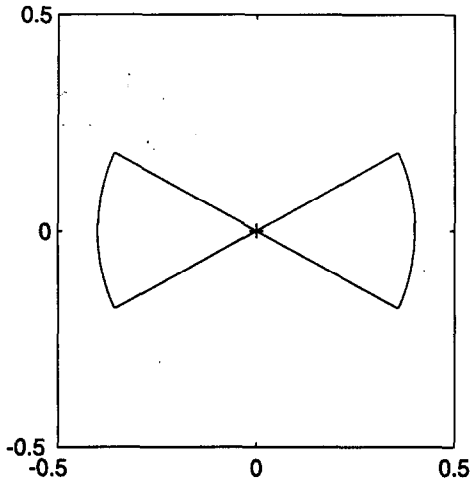

(a) $t_0 = 0$.

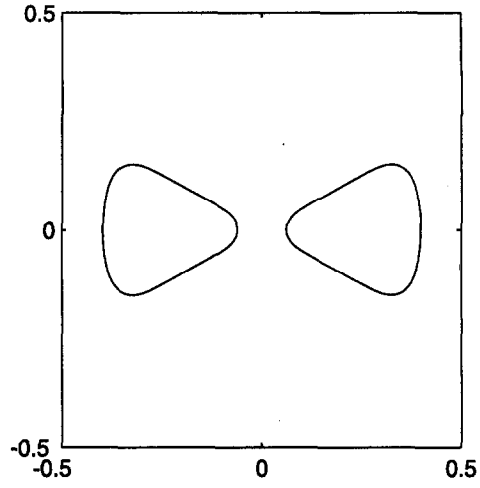

(b) $t_1 = 0.001$.

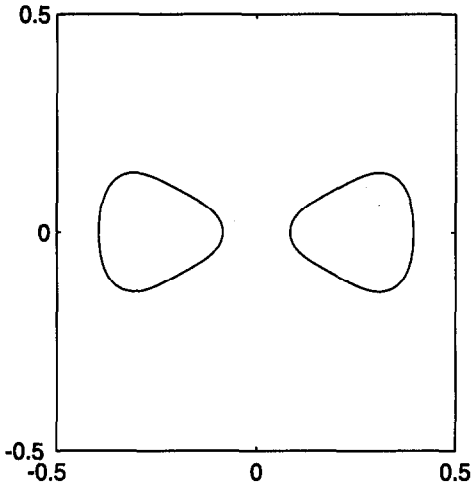

(c) $t_2 = 0.002$.

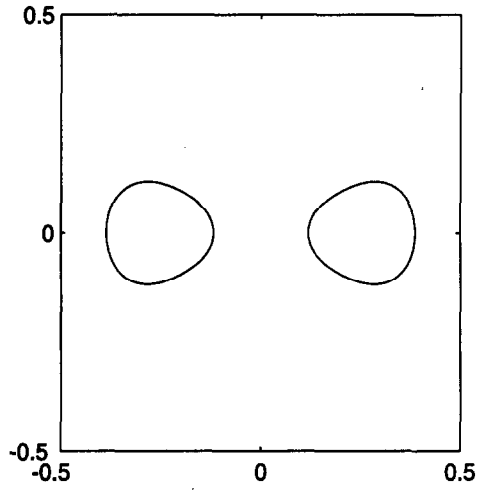

(d) $t_3 = 0.004$.

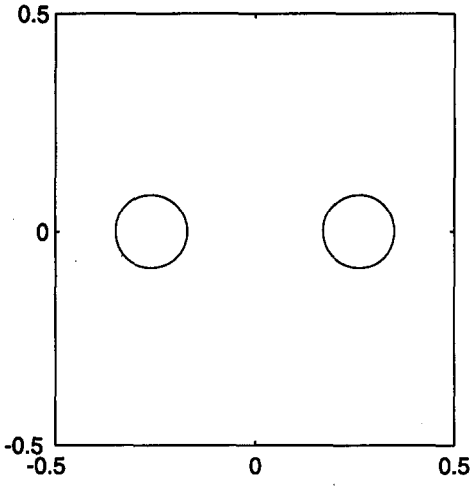

(e) $t_4 = 0.008$.

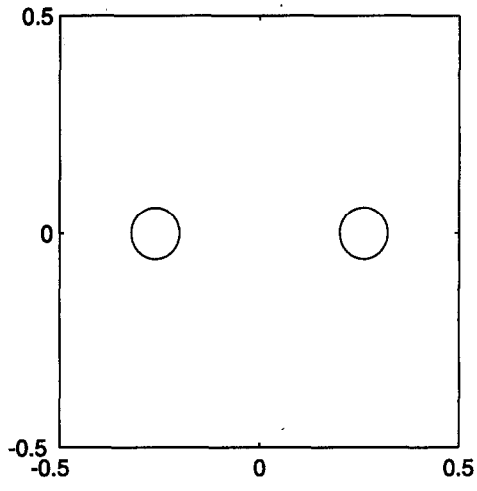

(f) $t_5 = 0.01$.

Figure 5. Numerical results for Example 4. '+' is the intersection point. $\alpha = 2\tan^{-1} 1/2 < \pi/2$. $\varepsilon = 0.01$, $h = 1/256$, $k = 0.0000025$.

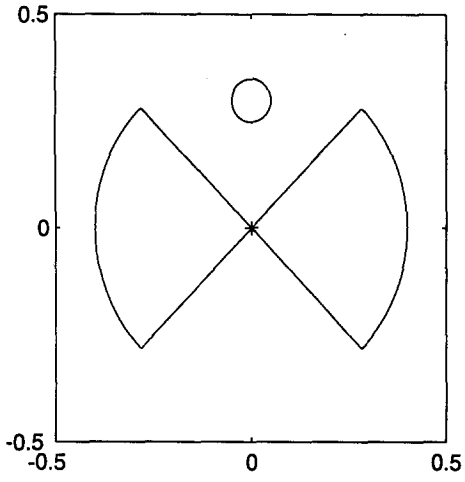

(a) $t_0 = 0$.

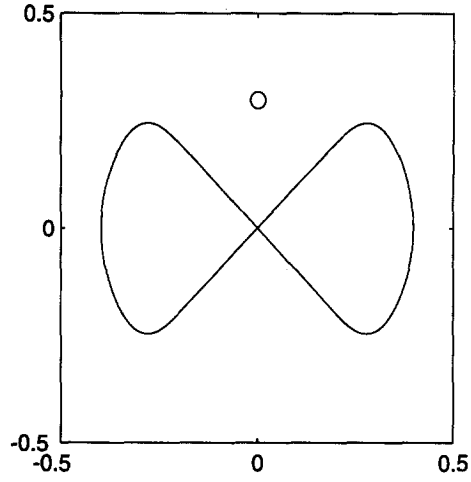

(b) $t_1 = 0.001$.

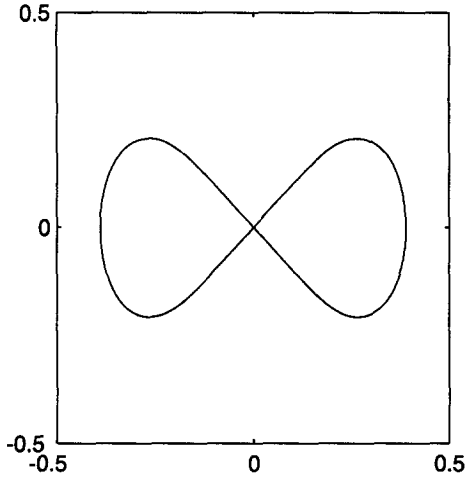

(c) $t_2 = 0.004$.

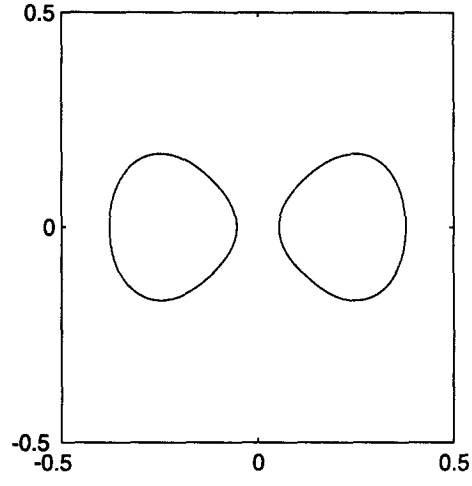

(d) $t_3 = 0.008$.

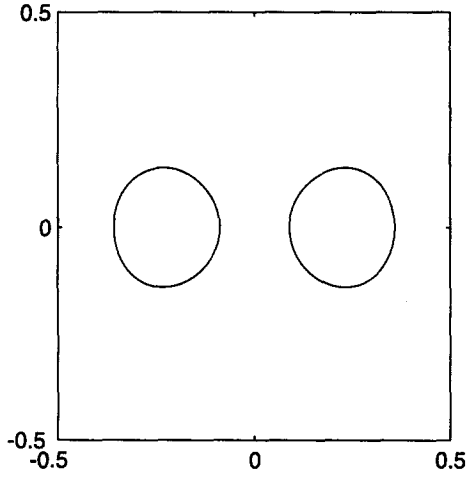

(e) $t_4 = 0.012$.

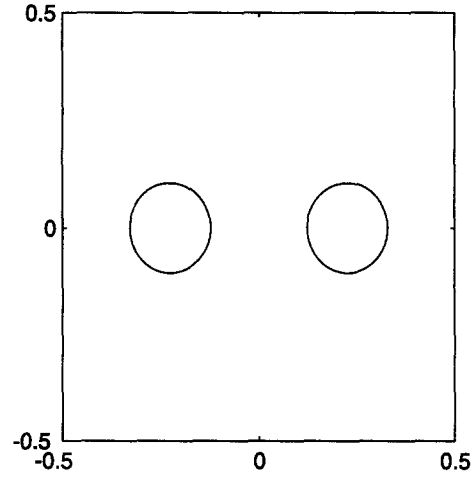

(f) $t_5 = 0.016$.

(i) $r_0 = 0.05$.

Figure 6. Numerical results for Example 5. '+' is the intersection point. $\alpha = \pi/2$. $\varepsilon = 0.01$, $h = 1/256$, $k = 0.0000025$.

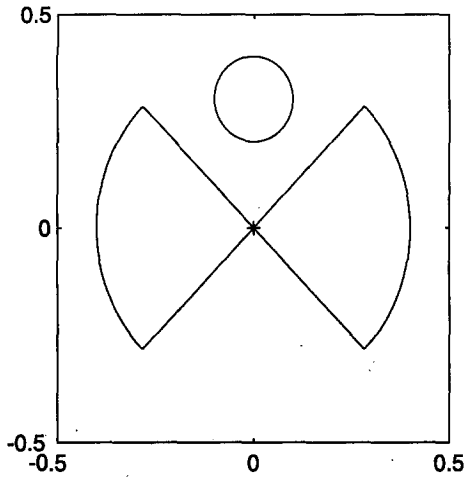

(a) $t_0 = 0$.

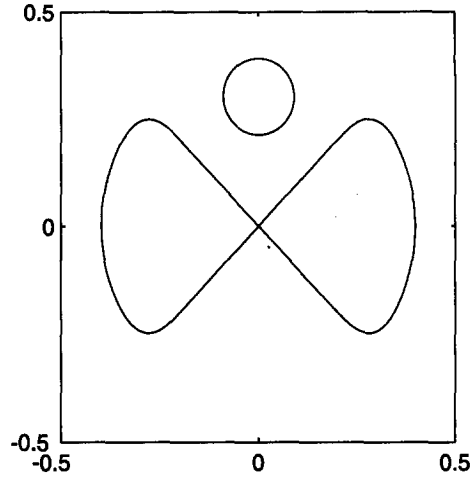

(b) $t_1 = 0.001$.

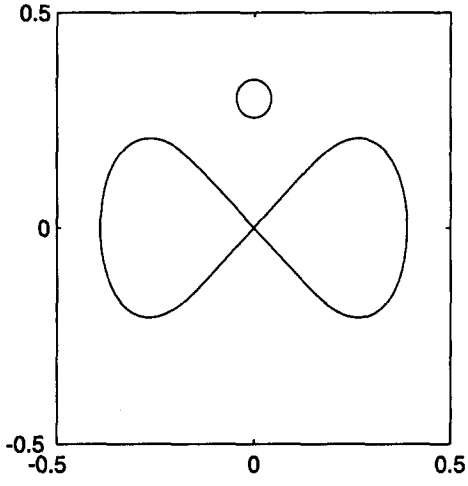

(c) $t_2 = 0.004$.

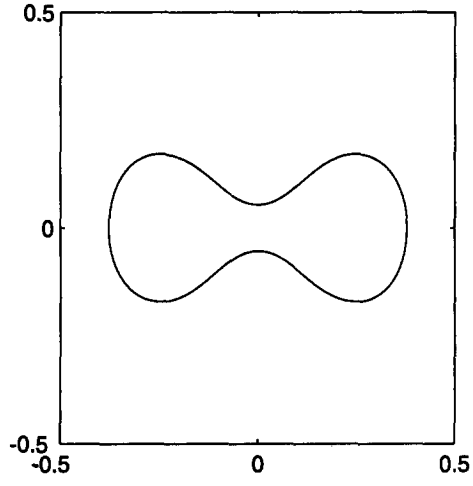

(d) $t_3 = 0.008$.

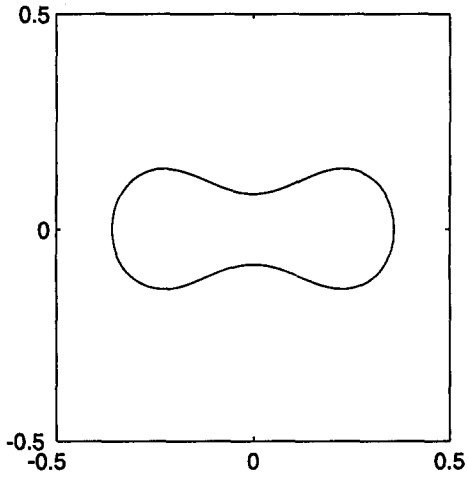

(e) $t_4 = 0.012$.

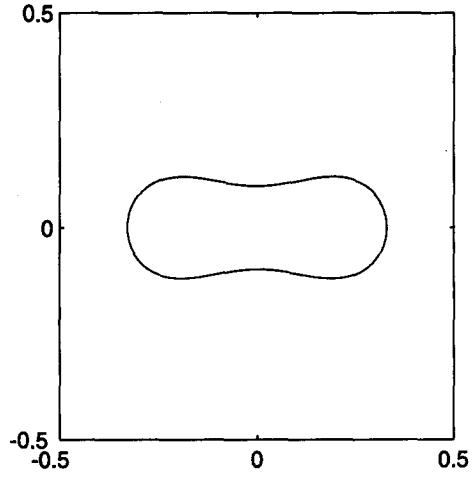

(f) $t_5 = 0.016$.

(ii) $r_0 = 0.1$.

Figure 6. (cont.)

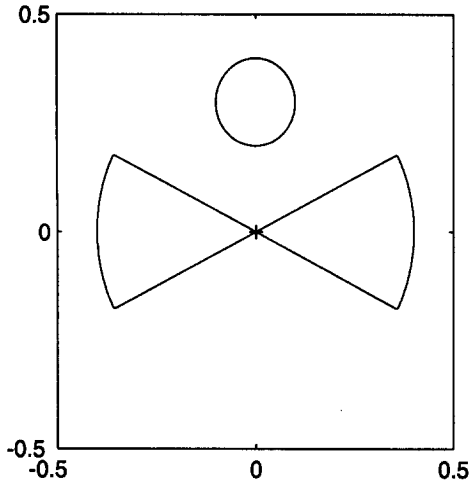

(a) $t_0 = 0$.

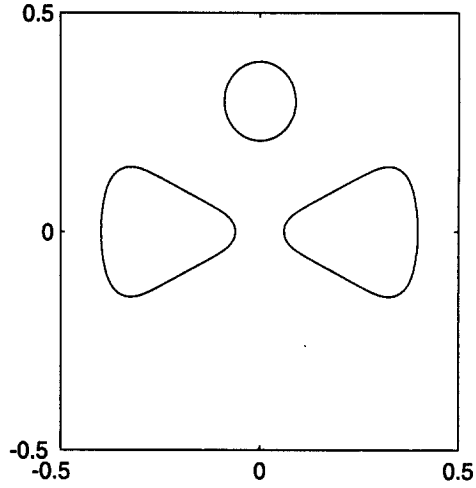

(b) $t_1 = 0.001$.

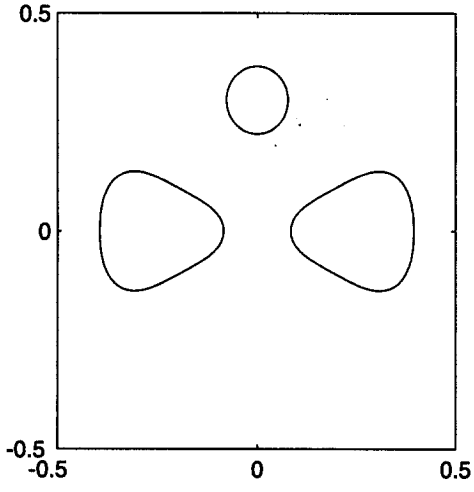

(c) $t_2 = 0.002$.

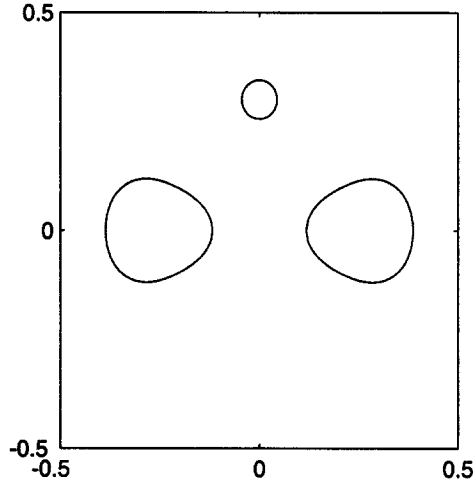

(d) $t_3 = 0.004$.

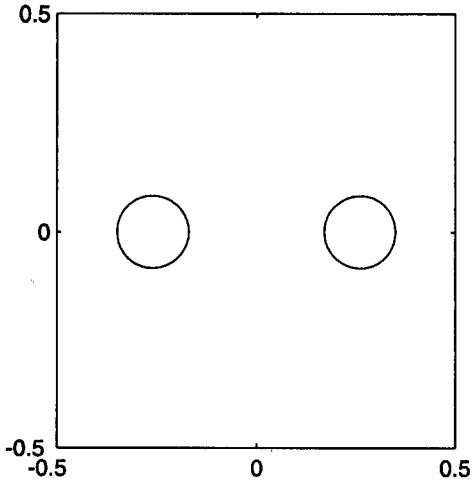

(e) $t_4 = 0.008$.

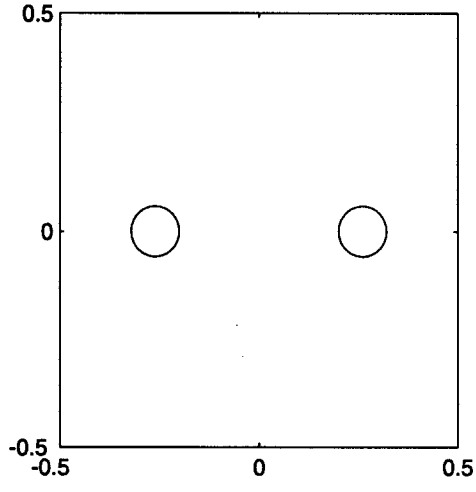

(f) $t_5 = 0.01$.

Figure 7. Numerical results for Example 6. '+' is the intersection point. $\alpha = 2\tan^{-1} 1/2 < \pi/2$, $r_0 = 0.1$. $\varepsilon = 0.01$, $h = 1/256$, $k = 0.0000025$.

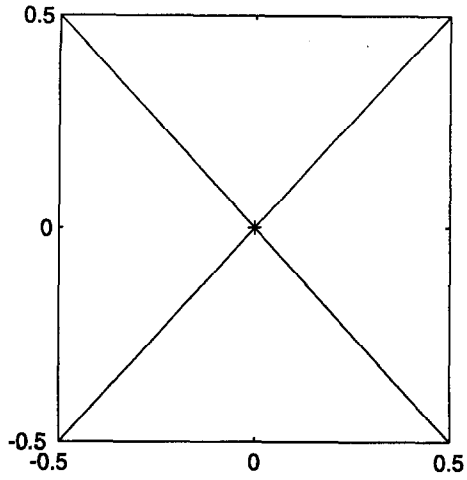

(a) $t_0 = 0$.

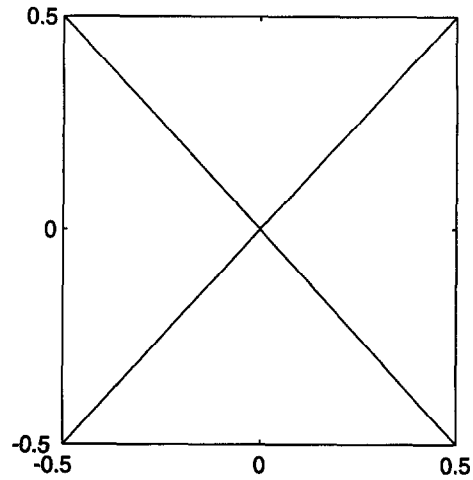

(b) $t_1 = 0.008$.

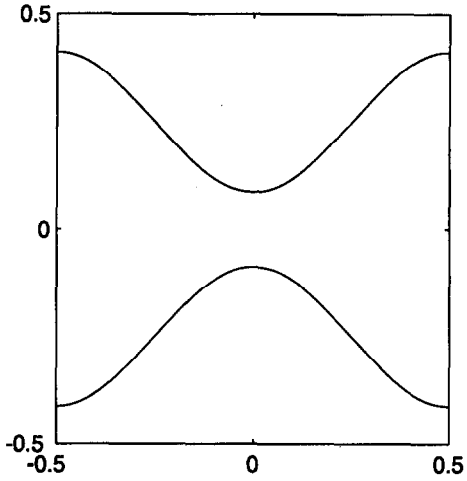

(c) $t_2 = 0.016$.

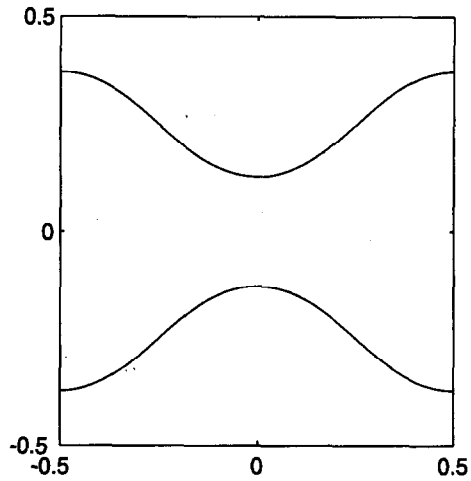

(d) $t_3 = 0.024$.

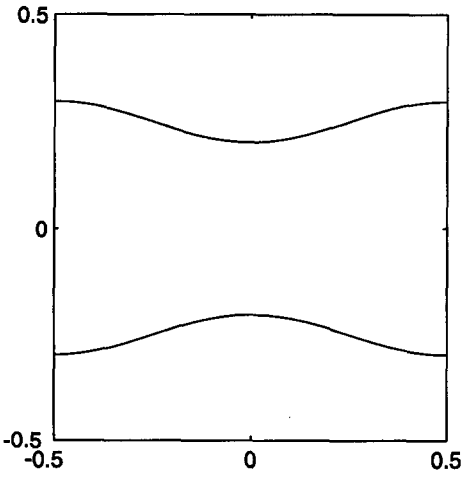

(e) $t_4 = 0.05$.

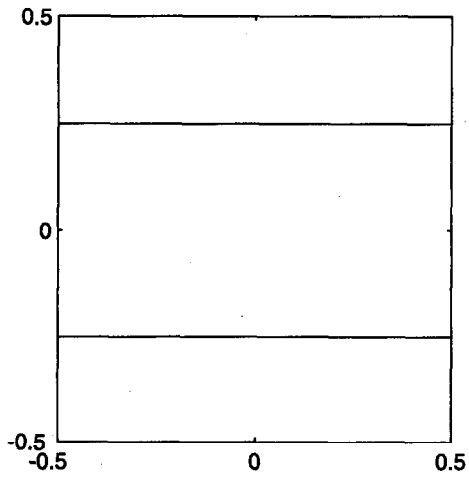

(f) $t_5 = 0.2$.

(i) $h = 1/256$, $k = 0.0000025$.

Figure 8. Numerical results for Example 7. '+' is the intersection point. $\alpha = \pi/2$, $\varepsilon = 0.01$.

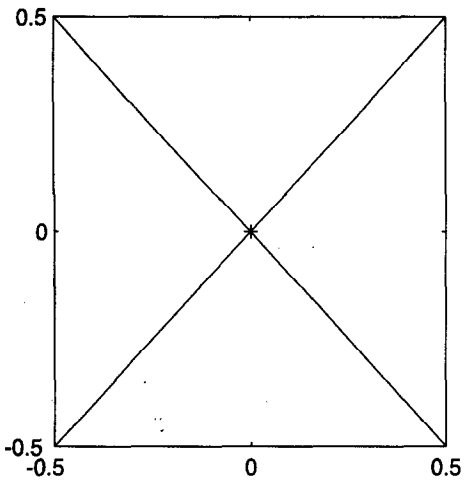

(a) $t_0 = 0$.

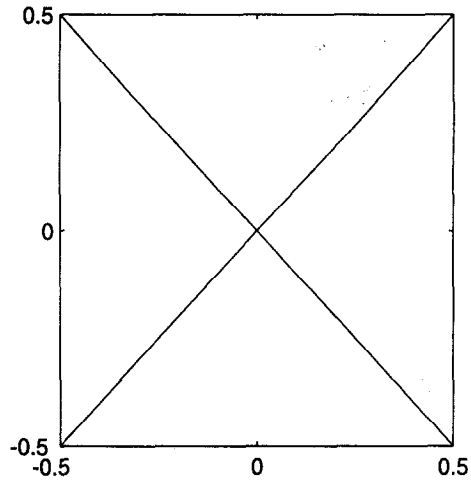

(b) $t_1 = 0.008$.

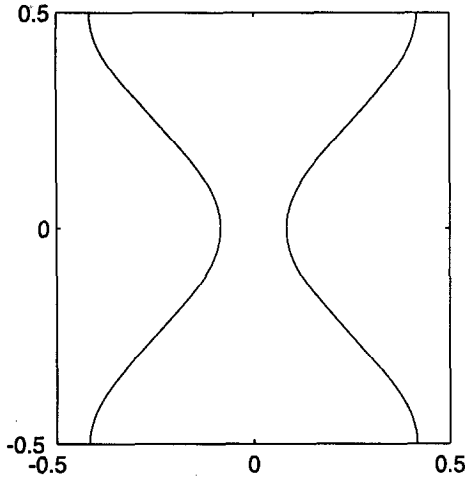

(c) $t_2 = 0.016$.

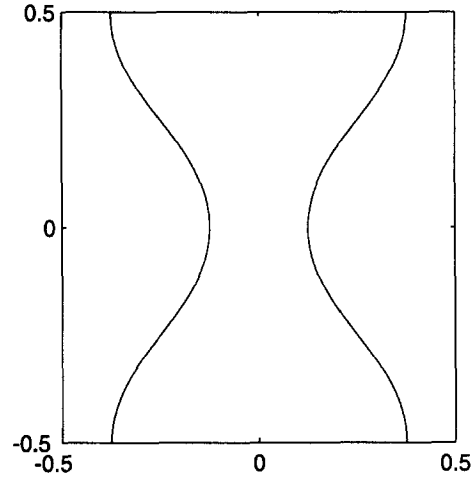

(d) $t_3 = 0.024$.

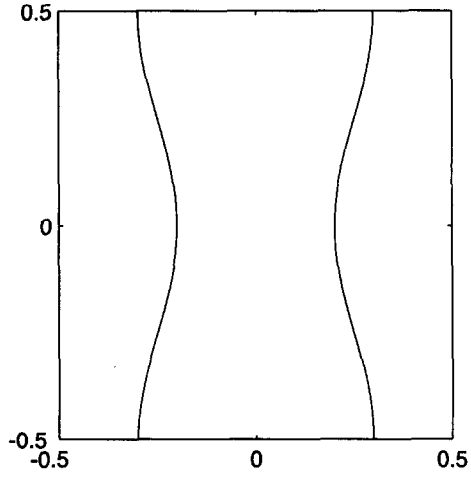

(e) $t_4 = 0.05$.

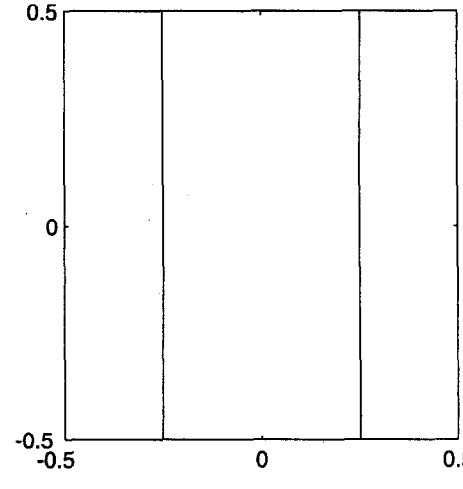

(f) $t_5 = 0.2$.

(ii) $h = 1/128$, $k = 0.00001$.

Figure 8. (cont.)

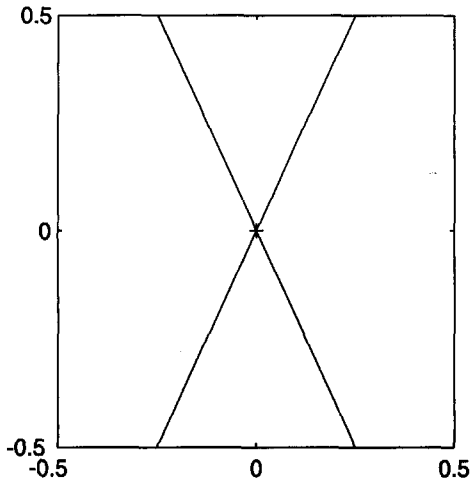

(a) $t_0 = 0$.

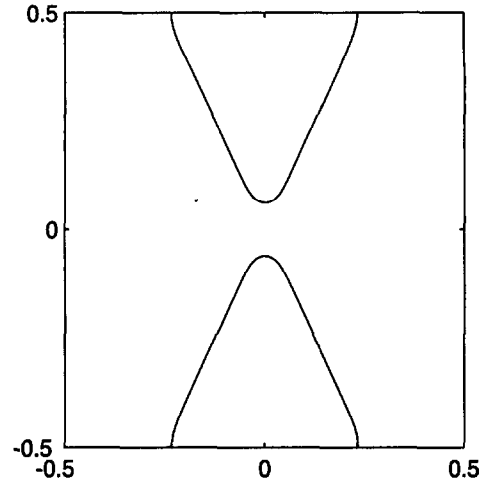

(b) $t_1 = 0.001$.

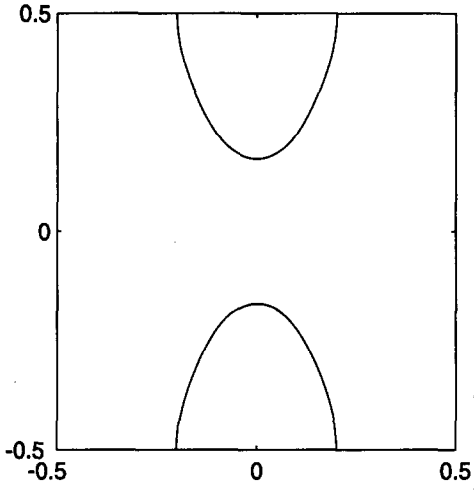

(c) $t_2 = 0.008$.

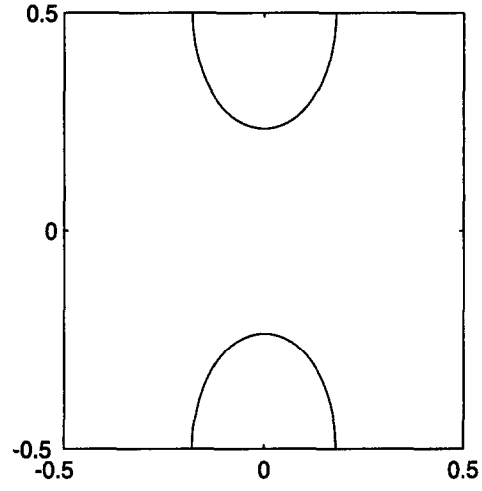

(d) $t_3 = 0.016$.

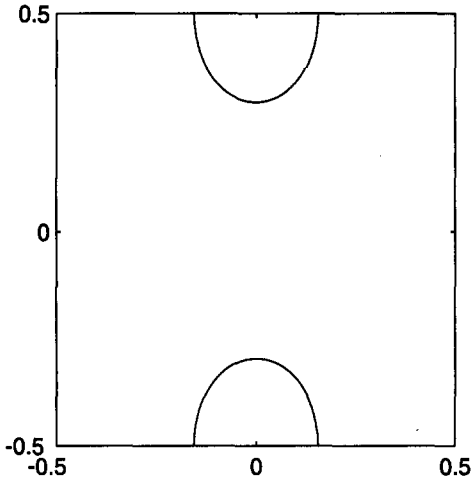

(e) $t_4 = 0.024$.

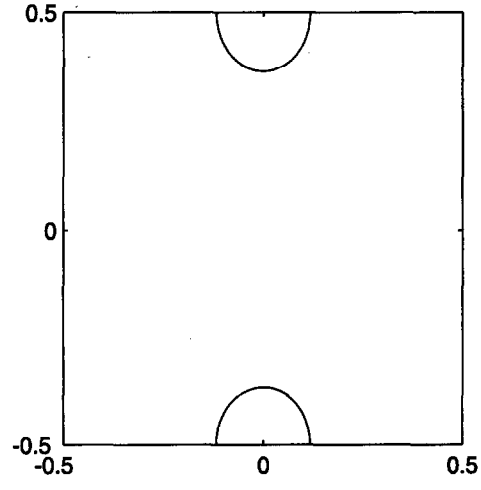

(f) $t_5 = 0.032$.

Figure 9. Numerical results for Example 8. '+' is the intersection point. $\alpha = 2\tan^{-1} 2 > \pi/2$, $\varepsilon = 0.01$, $h = 1/256$, $k = 0.0000025$.

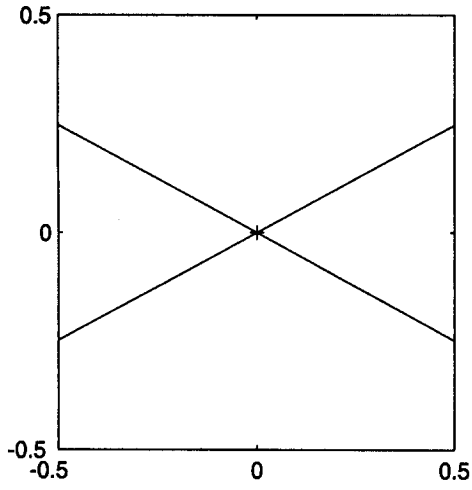

(a) $t_0 = 0$.

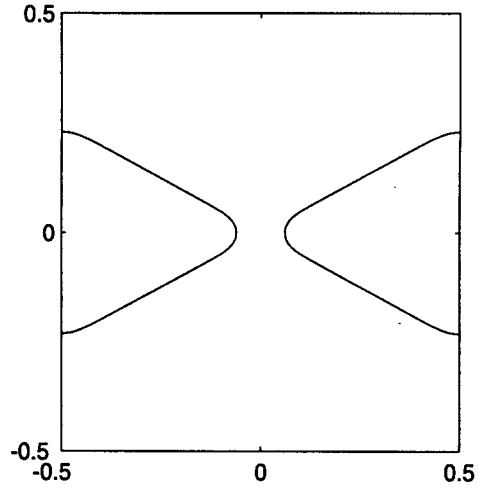

(b) $t_1 = 0.001$.

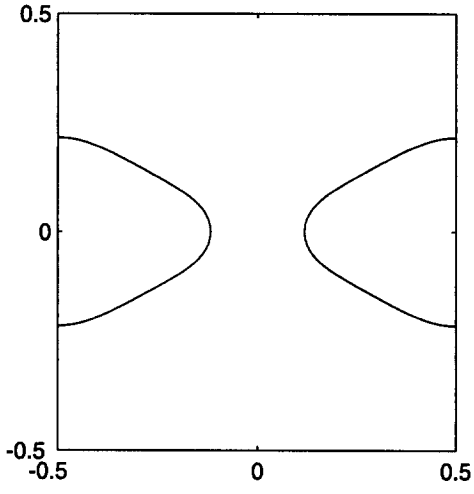

(c) $t_2 = 0.004$.

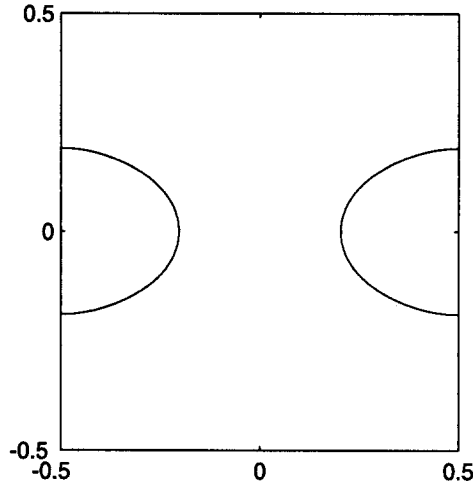

(d) $t_3 = 0.012$.

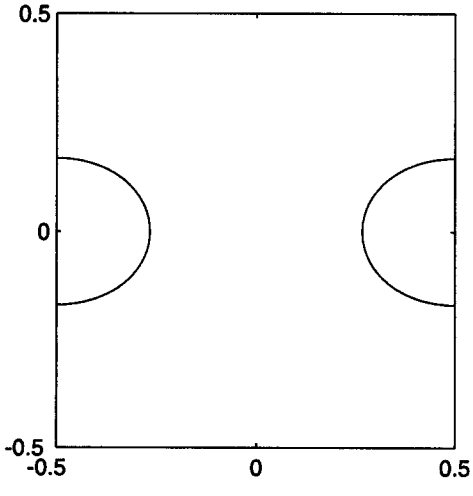

(e) $t_4 = 0.02$.

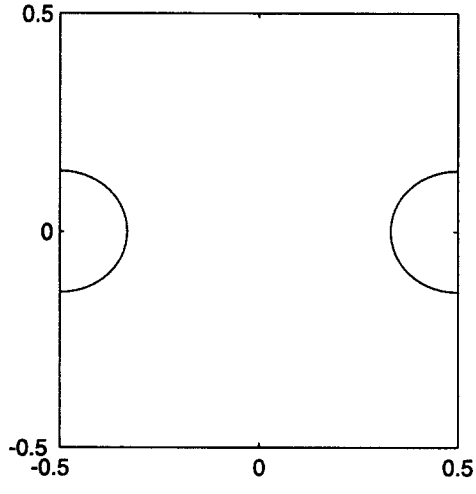

(f) $t_5 = 0.028$.

Figure 10. Numerical results for Example 9. '+' is the intersection point. $\alpha = 2\tan^{-1} 1/2 < \pi/2$, $\varepsilon = 0.01$, $h = 1/256$, $k = 0.0000025$.

EXAMPLE 7. Motion of a curve with two intersection segments and with an angle $\alpha = \pi/2$ at the intersection point. In this example and the next two, the plus (or minus) sign of the sign distance function in (2.3) is chosen if the point (x, y) is in left-right parts (or bottom-top parts) of the curve Γ_0. Figure 8 shows the motion of Γ_0 under its mean curvature at $t_0 = 0$, $t_1 = 0.008$, $t_2 = 0.016$, $t_3 = 0.024$, $t_4 = 0.05$, and $t_5 = 0.2$. From this figure, we can see Γ_0 splits at its intersection point either in the vertical direction or in the horizontal direction. Which direction to break up is due to the round-off error.

EXAMPLE 8. Motion of a curve with two intersection segments and with an angle $\alpha = 2\tan^{-1} 2 > \pi/2$ at the intersection point. Figure 9 shows the motion of Γ_0 under its mean curvature at $t_0 = 0$, $t_1 = 0.001$, $t_2 = 0.008$, $t_3 = 0.016$, $t_4 = 0.024$, and $t_5 = 0.032$. From this figure, we can see Γ_0 splits at its intersection point in the horizontal direction. In fact, from our numerical experiments, we find Γ_0 always splits at its intersection point in the horizontal direction when the angle $\alpha > \pi/2$.

EXAMPLE 9. Motion of a curve with two intersection segments and with an angle $\alpha = 2\tan^{-1} \times 1/2 < \pi/2$ at the intersection point. Figure 10 shows the motion of Γ_0 under its mean curvature at $t_0 = 0$, $t_1 = 0.001$, $t_2 = 0.004$, $t_3 = 0.012$, $t_4 = 0.02$, and $t_5 = 0.028$. From this figure, we can see Γ_0 splits at its intersection point in the vertical direction. In fact, from our numerical experiments, we find Γ_0 always splits at its intersection point in the vertical direction when the angle $\alpha < \pi/2$.

From Figures 3–10, we can see that which direction to split of the curve at the intersection point depends on the angle of the curve at the point, i.e., it splits in the horizontal direction when the angle $\alpha > \pi/2$, in vertical direction when $\alpha < \pi/2$, and in either direction when $\alpha = \pi/2$.

3. NONLOCAL EVOLUTION EQUATION WITH KAC POTENTIAL

In this section, we study numerically what happens for the nonlocal evolution equation with Kac potential when it is used to describe motion of a curve with intersection points under its mean curvature.

3.1. The Equation

Another model that is also commonly used in practice for the motion of Γ_0 under its mean curvature is the nonlocal evolution equation with Kac potential [6]

$$u_t = \frac{1}{\varepsilon^2}\left(-u + \tanh\left(\beta J^{(\varepsilon)} * u\right)\right), \qquad u(x, y, 0) = u_0(x, y), \tag{3.1}$$

where $\beta > 1$ is a positive constant, the initial function $u_0(x, y)$ is monotone near Γ_0, Γ_0 is the zero contour of $u_0(x, y)$, and $J^{(\varepsilon)}(x^2+y^2) = \varepsilon^{-2} J(\varepsilon^{-2}(x^2+y^2))$ with J the normalized Kac potential, i.e., $\int J(x, y)\, dx\, dy = 1$. Here we use the notation $J^{(\varepsilon)} * u$ to denote the convolution of $J^{(\varepsilon)}$ and u. The curve Γ_t, moved from Γ_0 under its mean curvature at time t, is the zero contour of the function $u(x, y, t)$. This model is obtained from the evolution of an Ising spin system with Kac potential J in the limit when the inverse range of the potential goes to 0. It describes the macroscopic behavior of the spin system with Kac potential and Glauber dynamics.

3.2. Discretization

We use forward Euler for time discretization, i.e.,

$$\begin{aligned} u_{ij}^{n+1} &= u_{ij}^n + \frac{k}{\varepsilon^2}\left[-u_{ij}^n + \tanh\left(\beta\left(J^{(\varepsilon)} * u^n\right)_{ij}\right)\right] \\ &= \left(1 - \frac{k}{\varepsilon^2}\right) u_{ij}^n + \frac{k}{\varepsilon^2}\tanh\left(\beta\left(J^{(\varepsilon)} * u^n\right)_{ij}\right), \end{aligned} \tag{3.2}$$

where the convolution $J^{(\varepsilon)} * u^n$ is computed by FFT. The mesh size h should resolve ε, i.e., $h < \varepsilon$. The stability condition is $k < 1/\varepsilon^2$.

The initial data is chosen as

$$u_0(x,y) = u_\beta \tanh\left(\pm \frac{d(x,y;\Gamma_0)}{\varepsilon}\right), \tag{3.3}$$

where $d(x,y;\Gamma_0)$ is the signed distance function and the constants $\pm u_\beta$ are stationary solution of (3.1), with u_β the strictly positive solution of

$$u_\beta = \tanh(\beta\, u_\beta). \tag{3.4}$$

3.3. Numerical Results

In the computation, we take the Kac potential as the Gaussian potential, i.e.,

$$J(x,y) = \frac{1}{4\pi} e^{-(x^2+y^2)/4}, \qquad J^{(\varepsilon)}(x,y) = \frac{1}{4\pi\varepsilon^2} e^{-(x^2+y^2)/4\varepsilon^2}, \tag{3.5}$$

and $\beta = 2.0$, thus, $m_\beta = 0.957504024$ (cf. (3.4)), and solve all the examples in Section 2 on $[-0.5, 0.5]^2$ with periodic boundary conditions. The mesh size is chosen as $h = 1/256$, $\varepsilon = 0.01$, and $k = 0.00005$.

From our numerical experiments, we find that the splitting pattern at the intersection points obtained by this model are the same as those obtained by the Allen-Cahn equation. Thus, the detail figures are omitted here.

4. CONCLUSION

We study numerically the motion of a curve with intersection points in the plane under its mean curvature by using the Allen-Cahn equation and the nonlocal evolution equation with Kac potential. The numerical results, i.e., splitting pattern at the intersection point, obtained from these two models are the same. From our numerical results, we find that which direction to split of the curve at the intersection point depends on the angle of the curve at that point, i.e., it splits in horizontal direction when the angle $\alpha > \pi/2$, in vertical direction when $\alpha < \pi/2$, and in either direction when $\alpha = \pi/2$. To study this splitting pattern mathematically is our future research interest.

REFERENCES

1. S. Osher and J. Sethian, Fronts propagating with curvature-dependent speed: Algorithms based on Hamilton-Jacobi formulations, *J. Comput. Phys.* **79**, 12–49, (1988).
2. J.A. Sethian, *Level Set Methods: Evolving Interfaces in Geometry, Fluid Mechanics, Computer Vision, and Materials Science*, Cambridge University Press, (1996).
3. S.M. Allen and J.W. Cahn, A macroscopic theory for antiphase boundary motion and its application to antiphase domain coarsening, *Acta Metal.* **27**, 1085–1095, (1979).
4. X. Chen, C.M. Elliott, A.R. Gardiner and J.J. Zhao, Convergence of numerical solutions to the Allen-Cahn equation, *Appl. Anal.* **69**, 47–56, (1998).
5. T. Ilmanen, Convergence of the Allen-Cahn equation to Brakke's motion by mean curvature, *J. Differential Geom.* **38**, 417–461, (1993).
6. A. De Masi, E. Orlandi, E. Presutti and L. Triolo, Motion by curvature by scaling nonlocal evolution equations, *J. Stat. Phys.* **73**, 543–570, (1993).
7. A. De Masi, E. Orlandi, E. Presutti and L. Triolo, Glauber evolution with the Kac potentials I: Mesoscopic and macroscopic limits, interface dynamics, *Nonlinearity* **7**, 633–696, (1994).
8. A. De Masi, E. Orlandi, E. Presutti and L. Triolo, Glauber evolution with the Kac potentials III: Spinodal decomposition, *Nonlinearity* **9**, 53–114, (1996).
9. M. Katsoulakis and P.E. Souganidis, Generalized motion by mean curvature as a macroscopic limit of stochastic Ising models with long range interactions and Glauber dynamics, *Comm. Math. Phys.* **169**, 61–97, (1995).
10. M. Katsoulakis and A.T. Kho, Stochastic curvature flows: Asymptotic derivation, level set formation and numerical experiments, *Interfaces Free Bound.* **3**, 265–290, (2001).

11. G.B. Ermentrout and L. Edelstein-Keshet, Cellular automata approaches to biological modeling, *J. Theoretical Biology* **160**, 97–133, (1993).
12. M. Gerhardt, H. Schuster and J.J. Tyson, A cellular automata model of excitable media II: Curvature, dispersion, rotating waves and meandering waves, *Physica D* **46**, 392–415, (1990).
13. M. Gerhardt, H. Schuster and J.J. Tyson, A cellular automata model of excitable media including curvature and dispersion, *Science* **247**, 416–425, (1990).
14. M. Markus and B. Hess, Isotropic cellular automaton for modeling excitable media, *Nature* **347**, 56–58, (1990).
15. P. Mascarenhas, Diffusion generated motion by mean curvature, CAM Report 92-23, University of California, Dept. of Math, Los Angeles, CA, (1992).
16. B. Merriman, J. Bence and S. Osher, Diffusion generated motion by mean curvature, CAM Report 92-18, University of California, Dept. of Math, Los Angeles, CA, (1992).
17. B. Merriman, J. Bence and S. Osher, Motion of multiple junctions: A level set approach, *J. Comput. Phys.* **112**, 334–363, (1994).
18. S.J. Ruuth, A diffusion-generated approach to multiphase motion, *J. Comput. Phys.* **145**, 166–192, (1998).
19. S.J. Ruuth, Efficient algorithms for diffusion-generated motion by mean curvature, *J. Comput. Phys.* **144**, 603–625, (1998).